Sleep Medicine 13 (2012) 102–106

Contents lists available at SciVerse ScienceDirect

Sleep Medicine

journal homepage: www.elsevier.com/locate/sleep

Brief Communication

Preclinical substantia nigra dysfunction in rapid eye movement sleep behaviour disorder

Masayuki Miyamoto [a,*], Tomoyuki Miyamoto [a], Masaoki Iwanami [a], Shin-ichi Muramatsu [b], Sayaka Asari [b], Imaharu Nakano [b], Koichi Hirata [a]

[a] Department of Neurology, Centre of Sleep Medicine, Dokkyo Medical University School of Medicine, Tochigi, Japan
[b] Division of Neurology, Department of Medicine, Jichi Medical University, Tochigi, Japan

ARTICLE INFO

Article history:
Received 10 November 2010
Received in revised form 22 January 2011
Accepted 17 March 2011
Available online 26 October 2011

Keywords:
REM sleep behaviour disorder
6-[^{18}F] Fluoro-meta-tyrosine (FMT) positron emission tomography
Transcranial sonography
Dopaminergic neurons
Parkinson's disease
Substantia nigra hyperechogenicity

ABSTRACT

Objectives: Transcranial sonography (TCS) has been shown to reveal hyperechogenicity of the substantia nigra (SN) in people with Parkinson's disease and in approximately 10% of healthy subjects. It is hypothesized that SN hyperechogenicity in healthy subjects and patients with idiopathic rapid eye movement (REM) sleep behaviour disorder (iRBD) patients is a marker of vulnerability for Parkinson's disease.
Methods: TCS and positron emission tomography (PET) with 6-[^{18}F] fluoro-meta-tyrosine (FMT), which can assess the level of the presynaptic dopaminergic nerve, were performed in 19 male patients with iRBD, mean age 66.4 (standard deviation [SD] 4.9) years, to assess nigrostriatal function.
Results: Nine patients had pathological SN hyperechogenicity (mean age 66.8 [SD 3.9] years; 0.31 [SD 0.12] cm^2) and 10 patients did not have SN hyperechogenicity (mean age 66.0 [SD 5.8] years; 0.11 [SD 0.06] cm^2). FMT uptake at the putamen and caudate was significantly lower in iRBD patients with pathological SN hyperechogenicity compared with those without SN hyperechogenicity. However, no correlation was found between SN echogenicity and FMT uptake. This is in conflict with previous findings which showed that subjects with hyperechogenicity had lower FMT uptake in the striatum.
Conclusion: Pathological hyperechogenic alterations in the SN in patients with iRBD may suggest the existence of preclinical SN dysfunction as determined by FMT-PET.

1. Introduction

Rapid eye movement (REM) sleep behaviour disorder (RBD) is a parasomnia characterised by dream-enacting behaviours, unpleasant dreams and lack of muscle atonia during REM sleep. RBD may be idiopathic or related to neurological disease [1]. Patients with idiopathic RBD (iRBD) have been reported to be at increased risk for developing Parkinson's disease (PD) [2]. Transcranial sonography (TCS) has been shown to reveal hyperechogenicity of the substantia nigra (SN) in patients with PD and in approximately 10% of healthy subjects, and has been suggested as a risk marker for PD in non-Parkinsonian subjects [3]. However, Berg et al. reported that SN hyperechogenicity in the elderly is non-specific and of limited usefulness in predicting an individual's risk for PD [4]. Recently, two case-control studies [5,6] showed that pathological SN hyperechogenicity was significantly more common in patients with iRBD compared to control subjects. iRBD is regarded as one of the non-motor symptoms of PD, and precedes motor symptoms. Schenck et al. identified the development of Parkinsonism in 11 of 29 men initially diagnosed with iRBD [7]. It is hypothesized that SN hyperechogenicity in healthy subjects and patients with iRBD is a vulnerability marker for PD. Although there is strong evidence that the echo originates from increased local iron content, the exact pathophysiological mechanisms for SN hyperechogenicity are not completely understood.

In order to verify the hypothesis that hyperechogenic alterations in the SN may be suggestive of preclinical nigrostriatal dopaminergic dysfunction for patients with iRBD, this study evaluated the presynaptic dopaminergic function in the striatum using 6-[^{18}F] fluoro-meta-tyrosine (FMT) positron emission tomography (PET).

2. Methods

This study was performed in accordance with the Declaration of Helsinki. Procedures were approved by the Ethics Review Committee of Dokkyo Medical University, and informed consent was obtained from each subject. TCS and 6-[^{18}F]FMT PET were performed in 19 males with iRBD confirmed by polysomnography.

* Corresponding author. Address: Dokkyo Medical University School of Medicine, 880 Kitakobayashi Mibu, Tochigi 321-0293, Japan. Tel.: +81 282 87 2152; fax: +81 282 86 5884.
E-mail address: miyamasa@dokkyomed.ac.jp (M. Miyamoto).

1389-9457/$ - see front matter © 2011 Elsevier B.V. All rights reserved.
doi:10.1016/j.sleep.2011.03.024

The mean age of subjects was 66.4 (standard deviation [SD] 4.9) years, the mean estimated duration of RBD was 3.5 (SD 1.8) years, the mean score on the Mini-Mental State Examination (MMSE) was 28.4 (SD 2.0), and the mean score on the Unified Parkinson's Disease Rating Scale (UPDRS) part III was 0.9 (SD 1) (range 0–3). Subjects were recruited from a sleep disorders clinic at Dokkyo Medical University Hospital between July 2008 and 2010. All had a history of recurrent dream-enacting behaviours, and RBD was diagnosed according to the International Classification of Sleep Disorders, second edition [8].

2.1. 6-[^{18}F] Fluoro-meta-tyrosine positron emission tomography

The PET radiotracer FMT is a substrate of the dopamine-synthesizing enzyme. Most FMT signals result from tracer that has been metabolized by aromatic amino acid decarboxylase (AADC) and monoamine oxidase-A, and is trapped in axon terminals as 6-fluoro-m-hydrophenylacetic acid without being released or further processed. FMT signals represent the extent of AADC activity more fully [9,10].

For 6-[^{18}F]FMT PET, the subject was placed on the scanner bed in a GEMINI-TF64 (Philips, Amsterdam, The Netherlands) in the supine position. 6-[^{18}F]FMT (weight × 0.12 mCi) was injected intravenously using a syringe pump. Carbidopa pretreatment was used (weight × 2.5 mg). A 10-min static scan was obtained 80 min following injection of 6-[^{18}F]FMT. 6-[^{18}F]FMT PET and magnetic resonance imaging (MRI) scans were fused using a Putamen Analyzer (WebNet Technology, Nasushiobara, Japan). Regions of interest were placed manually at the perimeters of the right/left putamen, caudate and cerebellum in MRI scans of the same subjects. Right/left putamen:cerebellum (putamen) or caudate:cerebellum (caudate) ratios of 6-[^{18}F]FMT-derived radioactivity were estimated. The sizes of the regions of interest were not fixed. Tissue concentrations of 6-[^{18}F]FMT-derived radioactivity (in mCi/cc) were adjusted for the dose per unit of body mass and expressed in units of mCi-kg/cc-mCi (Fig. 1A and B).

2.2. Transcranial sonography

TCS was performed using a conventional transcranial Doppler sonograph equipped with a 2.5-MHz phased-array transducer as described previously [5]. Hyperechogenic areas on both sides were analysed separately. To compare areas of echogenicity and the frequency of hyperechogenicity, the side of the midbrain (right or left) with the greater area of SN echogenicity in each subject was used for these statistical comparisons. Planimetric quantification of the areas of increased echogenicity was done on both sides of the SN independently (Fig. 1C and D). In accordance with previously reported cut-off values, areas of echogenicity <0.20 cm^2 were classified as normal, and areas of echogenicity ⩾0.20 cm^2 were classified as pathological [3].

The mean interval between performance of TCS and FMT-PET was 126.6 (SD 174.8) days. TCS is performed routinely to assess preclinical condition at the study institute. Berg et al. reported that the echogenic area of the SN did not change in the course of PD during a 5-year follow-up study [11]. Therefore, the interval between the performance of TCS and FMT-PET cannot be considered to influence the results.

Clinical examinations, including the MMSE and UPDRS, FMT-PET and TCS were performed independently by physicians who were blinded to the results of other examinations.

2.3. Statistical analysis

Values are expressed as mean (SD). p-values were determined using the Mann–Whitney U-test. A p-value <0.05 was taken to indicate statistical significance. A statistical comparison of factors such as age of patients, MMSE score, UPDRS part III score and 6-[^{18}F]FMT uptake was performed between the groups of patients with iRBD based on the presence or absence of pathological SN hyperechogenicity. The Spearman's correlation coefficient was used for analysis of the correlation between the echogenic area of the SN and the degree of 6-[^{18}F]FMT uptake.

3. Results

Demographic and clinical data on patients with iRBD are summarized in Table 1. Nine of the patients with iRBD had pathological SN hyperechogenicity (mean 0.31 [SD 0.12] cm^2) and 10 did not have SN hyperechogenicity (mean 0.11 [SD 0.06] cm^2). Therefore, the 19 patients were divided into two groups: those with and those without SN hyperechogenicity. Age distributions, MMSE scores, and UPDRS part III scores did not differ significantly between the groups. Evaluation of motor activity using the UPDRS part III score ranged from zero to three points, which did not fulfill the diagnostic criteria for probable PD. Compared with the patients without SN hyperechogenicity, the patients with SN hyperechogenicity had significantly lower uptake of 6-[^{18}F]FMT in the putamen (mean 4.40 [SD 0.83] and 3.22 [SD 0.98], respectively; $p = 0.027$) and the caudate (mean 3.69 [SD 0.42] and 2.86 [SD 0.82], respectively; $p = 0.014$) (Table 1). However, the echogenic area of the SN did not correlate with the degree of 6-[^{18}F]FMT uptake in the putamen ($r = -0.4465$, $p = 0.0553$) or the caudate ($r = -0.4007$, $p = 0.0891$). In addition, the UPDRS part III scores did not correlate with the degree of 6-[^{18}F]FMT uptake in the putamen ($r = -0.240$, $p = 0.323$), the caudate ($r = -0.040$, $p = 0.871$), or the echogenic area of the SN ($r = -0.216$, $p = 0.375$).

4. Discussion

Unger et al. [12] identified a significant association between midbrain hyperechogenicity and iRBD, and reported that two out of five iRBD patients with SN hyperechogenicity had unremarkable findings by presynaptic dopamine transporter imaging with fluoropropyl-carbomethoxy-iodophenyl-tropane (FP-CIT) single-photon emission computed tomography (SPECT). Iranzo et al. [13] recently reported that ^{123}I-FP-CIT striatal binding did not correlate with the extent of SN echogenicity in patients with iRBD. In the present study, FMT uptake in the putamen and caudate was significantly lower in iRBD patients with pathological SN hyperechogenicity than in those without SN hyperechogenicity. In contrast to the present results, Iranzo et al. [13] found that patients with SN hyperechogenicity did not have lower tracer uptake compared with patients without SN hyperechogenicity and they did not find a correlation between SN size and tracer uptake.

Booij et al. [14] reported that motor signs of PD started when the decrease in the percentage of ^{123}I-FP-CIT binding ratios in the putamen was 46–64% using age-corrected data. Spiegel et al. [15] and Doepp et al. [16] reported a lack of correlation between SN echogenicity and striatal FP-CIT uptake in patients with PD. Spiegel et al. [15] hypothesized that the pathogenic substrate of SN hyperechogenicity is different from that associated with degeneration of dopaminergic SN projection neurons. Berg et al. [11] failed to find evidence of an increase in the size of the echogenic SN area in a 5-year longitudinal study on PD patients with substantial progression of motor symptoms.

On the other hand, Weise et al. [17] reported a significant correlation between the extension of the echogenic SN area and striatal β-CIT binding. They discussed the possibility that the extension of SN echogenicity may be a consequence of degeneration of dopaminergic neurons in the SN, rather than an independent and

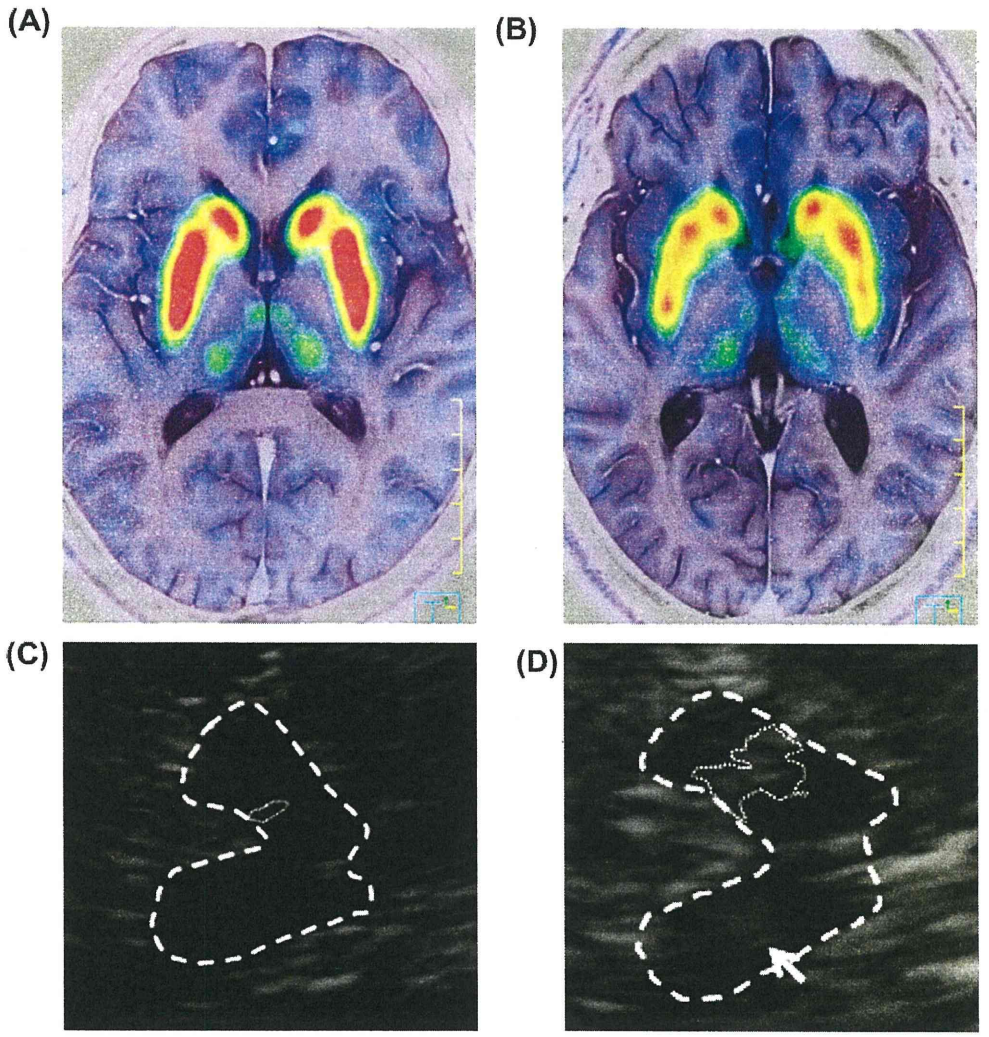

Fig. 1. (A) 6-[^{18}F] Fluoro-meta-tyrosine positron emission tomography (6-[^{18}F]FMT PET) on magnetic resonance imaging (MRI). This demonstrates preserved dopamine terminals in the caudate and putamen in a healthy subject. (B) 6-[^{18}F]FMT PET on MRI. This demonstrates patchy decreased dopamine terminals in the caudate and putamen in a patient with idiopathic rapid eye movement sleep behaviour disorder (iRBD). (C) Transcranial sonography (TCS) of bilateral substantia nigra (SN) hyperechogenicity in a healthy subject. The area of hyperechogenic SN signal within the hypo-echogenic crus cerebri is encircled on the ipsilateral side for planimetric measurement (0.10 cm^2). (D) TCS of bilateral SN hyperechogenicity in a patient with iRBD. The area of the hyperechogenic SN signal within the hypo-echogenic crus cerebri is encircled on the ipsilateral side for planimetric measurement (0.44 cm^2).

Table 1
Area of hyperechogenic substantia nigra (SN) signals in two groups of patients with idiopathic rapid eye movement sleep behaviour disorder (n = 19).

	SN hyperechogenicity*		p-Value
	Normal (<0.20 cm^2) (n = 10)	Pathological (⩾0.20 cm^2) (n = 9)	
Age (years), mean (SD)	66.0 (5.8)	66.8 (3.9)	0.623
Range, years	58–77	62–72	N/A
Sex, male/female	10/0	9/0	N/A
Estimated duration of RBD (years), mean (SD)	3.9 (1.7)	4.3 (2.1)	0.389
MMSE score, mean (SD)	28.4 (2.1)	28.4 (1.9)	0.864
UPDRS part III score, mean (SD)	0.9 (1.1)	1.0 (1.0)	0.729
Uptake of 6-[^{18}F] FMT, mean (SD)			
Putamen	4.40 (0.83)	3.22 (0.98)	0.027
Caudate	3.69 (0.42)	2.86 (0.82)	0.014
Putamen/caudate ratio	1.19 (0.19)	1.12 (0.10)	0.514

RBD, rapid eye movement sleep behaviour disorder; MMSE, Mini-Mental State Examination; UPDRS, Unified Parkinson's Disease Rating Scale; FMT, fluoro-meta-tyrosine; SD, standard deviation; N/A, not applicable.
Transcranial sonography (TCS) was considered pathological when SN echogenicity was ⩾0.20 cm^2.
p-Value was determined by Mann–Whitney U-test.
*Side of the midbrain (right or left) with the greater area of SN echogenicity.

mechanistically unrelated phenomenon. SN echogenicity is sensitive to degeneration of dopaminergic neurons. A report by Behnke et al. [18] showed that ^{18}fluoro-DOPA uptake was lowest in patients with PD, followed by individuals with SN hyperechogenicity, and finally healthy controls without SN hyperechogenicity. The difference was significant between the three groups. Walter et al. [19] reported that brain parenchyma sonography demonstrated SN hyperechogenicity in concordance with abnormal nigrostriatal ^{18}F-DOPA PET in all symptomatic and three asymptomatic *Parkin* mutation carriers. Thus, they suggested SN hyperechogenicity as an early marker for detection of preclinical Parkinsonism. DelleDonne et al. [20] showed that incidental Lewy body disease (ILBD) has nigrostriatal pathological features that are intermediate between those in pathologically normal persons and patients with PD. Among the participants with ILBD, decreased striatal dopaminergic immunoreactivity was documented for both tyrosine hydroxylase and vesicular monoamine transporter 2 in comparison with the pathologically normal subjects; the reductions were even greater in patients with PD. Also, SN neuronal loss correlated with both striatal vesicular monoamine transporter 2 and tyrosine hydroxylase. Thus, ILBD probably represents presymptomatic PD rather than non-specific, age-related α-synuclein pathological changes.

The current study compared FMT-PET findings in patients with iRBD with and without SN hyperechogenicity. Pathological SN hyperechogenicity in iRBD may be suggestive of nigrostriatal dopaminergic dysfunction, as determined by FMT-PET. However, there was no significant correlation between the area of SN hyperechogenicity and the degree of 6-[^{18}F]FMT uptake. It may be that these two parameters have different characteristics. In other words, the area of SN echogenicity is thought to be a stable marker, whereas the uptake of dopaminergic tracer changes progressively with time.

Iranzo et al. found that 19% of 43 patients developed a neurodegenerative syndrome such as PD, dementia with Lewy bodies (DLB), or multiple system atrophy (MSA) 2.5 years after TCS and ^{123}I-FP-CIT SPECT. They postulated that the combined use of ^{123}I-FP-CIT SPECT and TCS is a potential strategy for early identification of patients with iRBD who are at risk for development of a synucleinopathy [13]. They also reported that one case of iRBD who developed MSA had decreased striatal ^{123}I-FP-CIT uptake and normal echogenic SN, and this discrepancy might be explained by the fact that SN hyperechogenicity is less common in MSA than in PD or DLB [13]. Even when SN echogenicity is normal in iRBD, the risk for developing MSA remains. Therefore, patients with iRBD who are at risk for developing not only PD or DLB, but also MSA need to be followed-up.

This study had several limitations. One weak point was that the mean interval between TCS and FMT-PET was approximately four months. Berg et al. reported that the area of SN echogenicity did not change with time in PD [11], but this has not been investigated in patients with iRBD. Due to the lack of a control group in this study, it was not possible to assess if those patients with abnormal PET results had a greater or different echogenic size than those with normal PET results. Satisfactory results of TCS are difficult to obtain in females [5], and all subjects in the study were male. In the future, in order to clarify whether there is a gender difference in the relationship between SN hyperechogenicity and FMT-PET findings, it may be helpful to determine the background of the gender differences in the onset of PD.

Hyperechogenic alterations in the SN may suggest the existence of preclinical SN dysfunction and of an underlying neurodegenerative disorder such as PD or DLB associated with nigrostriatal dysfunction in patients with iRBD. In terms of clinical interest and use of the study findings, there is a need for close clinical follow-up to detect the early signs of a disease characterised by Parkinsonism, and also to test neuroprotective therapies in the near future in such patients.

Financial disclosure

This work was supported by Grants-in-Aid from the Research Committee of CNS Degenerative Diseases, the Ministry of Health, Labour and Welfare of Japan.

Conflict of interest

The ICMJE Uniform Disclosure Form for Potential Conflicts of Interest associated with this article can be viewed by clicking on the following link: doi:10.1016/j.sleep.2011.03.024.

Acknowledgements

The authors wish to thank their colleagues, particularly Y. Inoue (Japan Somnology Centre, Neuropsychiatry Research Institute and Department of Somnology, Tokyo Medical University). The authors also thank Dr. Masaya Segawa (Segawa Neurological Clinic for Children) for reviewing and commenting on the manuscript, and Junichi Saitou and Toshihiko Satou (PET Centre, Utsunomiya Central Clinic) for their technical support in performing FMT-PET.

References

[1] Boeve BF. REM sleep behavior disorder: updated review of the core features, the REM sleep behavior disorder-neurodegenerative disease association, evolving concepts, controversies, and future directions. Ann NY Acad Sci 2009;1184:15–54.
[2] Postuma RB, Lang AE, Massicotte-Marquez J, Montplaisir J. Potential early markers of Parkinson's disease in idiopathic REM sleep behavior disorder. Neurology 2006;66:845–51.
[3] Berg D. Transcranial ultrasound as a risk marker for Parkinson's disease. Mov Disord 2009;24:S677–83.
[4] Berg D, Seppi K, Liepelt I, et al. Enlarged hyperechogenic substantia nigra is related to motor performance and olfaction in the elderly. Mov Disord 2010;25:1464–9.
[5] Iwanami M, Miyamoto T, Miyamoto M, Hirata K, Takada E. Relevance of substantia nigra hyperechogenicity and reduced odor identification in idiopathic REM sleep behavior disorder. Sleep Med 2010;11:361–5.
[6] Stockner H, Iranzo A, Seppi K, et al. Midbrain hyperechogenicity in idiopathic REM sleep behavior disorder. Mov Disord 2009;24:1906–9.
[7] Schenck CH, Bundlie SR, Mahowald MW. Delayed emergence of a parkinsonian disorder in 38% of 29 older men initially diagnosed with idiopathic rapid eye movement sleep behavior disorder. Neurology 1996;46:388–93.
[8] American Academy of Sleep Medicine. International Classification OF Sleep Disorders. 2nd ed. Diagnosis and coding manual. Westcheste, IL: American Academy of Sleep Medicine; 2005. p. 148–52.
[9] Braskie MN, Wilcox CE, Landau SM, et al. Relationship of striatal dopamine synthesis capacity to age and cognition. J Neurosci 2008;28:14320–8.
[10] Muramatsu S, Fujimoto K, Kato S, et al. A phase I study of aromatic L-amino acid decarboxylase gene therapy for Parkinson's disease. Mol Ther 2010;18:1731–5.
[11] Berg D, Merz B, Reiners K, Naumann M, Becker G. Five-year follow-up study of hyperechogenicity of the substantia nigra in Parkinson's disease. Mov Disord 2005;20:383–5.
[12] Unger MM, Möller JC, Stiasny-Kolster K, et al. Assessment of idiopathic rapid-eye-movement sleep behavior disorder by transcranial sonography, olfactory function test, and FP-CIT-SPECT. Mov Disord 2008;23:596–9.
[13] Iranzo A, Lomena F, Stockner H, et al. Decreased striatal dopamine transporter uptake and substantia nigra hyperechogenicity as risk markers of synucleinopathy in patients with idiopathic rapid-eye-movement sleep behaviour disorder: a prospective study. Lancet Neurol 2010;9:1070–7.
[14] Booij J, Bergmans P, Winogrodzka A, Speelman JD, Wolters EC. Imaging of dopamine transporters with [^{123}I]FP-CIT SPECT does not suggest a significant effect of age on the symptomatic threshold of disease in Parkinson's disease. Synapse 2001;39:101–8.
[15] Spiegel J, Hellwig D, Mollers M, et al. Transcranial sonography and [^{123}I]FP-CIT SPECT disclose complementary aspects of Parkinson's disease. Brain 2006;129:118–9.
[16] Doepp F, Plotkin M, Siegel L, et al. Brain parenchyma sonography and ^{123}I-FP-CIT SPECT in Parkinson's disease and essential tremor. Mov Disord 2008;23:405–10.

[17] Weise D, Lorenz R, Schliesser M, Schirbel A, Reiners K, Classen J. Substantia nigra echogenicity: a structural correlate of functional impairment of the dopaminergic striatal projection in Parkinson's disease. Mov Disord 2009;24:1669–75.
[18] Behnke S, Schroeder U, Dillmann U, et al. Hyperechogenicity of the substantia nigra in healthy controls is related to MRI changes and to neuronal loss as determined by F-Dopa PET. NeuroImage 2009;47:1237–43.
[19] Walter U, Klein C, Hilker R, Benecke R, Pramstaller PP, Dressler D. Brain parenchyma sonography detects preclinical parkinsonism. Mov Disord 2004;19:1445–9.
[20] DelleDonne A, Klos KJ, Fujishiro H, et al. Incidental Lewy body disease and preclinical Parkinson disease. Arch Neurol 2008;65:1074–8.

＜原　著＞

Telestroke の有用性と課題

相澤　仁志[1)2)]　澤田　潤[1)]　齋藤　司[1)]　遠藤　寿子[1)]　片山　隆行[1)]
長谷部直幸[1)]　平沼　初音[3)]　高橋　康二[3)]　羽根田　俊[4)]　守屋　潔[5)]

要旨：【目的】脳卒中専門医不在の地域基幹病院において遠隔脳卒中診療(telestroke)を試み，その有用性と課題を検証する．【方法】脳卒中専門医チームを有する医療機関と脳卒中専門医不在の地域基幹病院をTV会議システムと放射線画像読影システムで結んだ．地域基幹病院に脳卒中を疑われた患者が搬送されたとき，TV会議システムを用いて得られた神経所見と放射線画像読影システムで転送された画像所見から，臨床診断し，治療方針を決定した．Telestrokeによる脳卒中診療の有用性および課題を検討した．【結果】Telestrokeにより患者の意識状態や麻痺の状態などを直接観察することができた．地域基幹病院で撮影した神経画像をリアルタイムで読影できた．脳卒中専門医のいる医療機関に直接搬送されるときより診断までの時間，治療開始までの時間が短縮した．診療点数が算定されないことが課題であった．【結論】Telestrokeは脳卒中専門医のいない地域基幹病院での脳卒中診療に有用と考えられた．

Key words：telestroke, stroke telemedicine, TV conferencing system
(脳卒中 33：84-88，2011)

はじめに

北海道は一つの医療圏が広く，また脳卒中を専門とする神経内科医や脳神経外科医が不在の地域が数多く存在する．したがって，このような地域では脳卒中急性期に専門医による適切な診療を受ける機会を逸することが予測される．一方，stroke unitを利用した脳卒中専門チームによる治療を行うことにより脳卒中患者の死亡率減少，機能予後改善が得られることが知られており[1)~3)]，脳卒中専門医不在の地域の脳卒中診療のレベルを維持し，脳卒中診療の地域差を解消する取り組みはきわめて重要と考えられる．このような観点から，1990年代の終わりから2000年にかけて欧米では脳卒中センターから遠隔地の脳卒中急性期患者にtissue plasminogen activator(t-PA)の使用を主な目的としてstroke telemedicine(telestroke)が発達してきた[5)]．そこで，本邦でも脳卒中専門医不在の地域基幹病院で遠隔脳卒中診療(telestroke)を試み，その有用性と課題を検証することを目的とした．

方　法

旭川医科大学では脳卒中診療レベルの向上と標準化のため2005年12月に神経内科と脳神経外科，循環器内科，救急部，放射線科などがストロークチームを結成した．主に神経内科と脳神経外科の脳卒中専門医が脳卒中の初期対応を行い，毎週合同ファレンスを行っている．旭川医科大学病院ストロークチームと脳卒中専門医不在の地域基幹病院(富良野病院)救急室をTV会議システム(video-conferencing system)で結んだ．脳卒中患者が富良野病院へ搬送された時に，旭川医科大学の脳卒中専門医がTV会議システムを用い救急搬送されたベッド上の患者のバイタルサイン，意識状態，神経所見を富良野病院の救急担当医と確認するようにした．TV会議システムは専用の光回線により結んで，リアルタイムで患者の状態を確認できるようにした(図1，2)．

1)旭川医科大学神経内科
2)現独立行政法人国立病院機構東京病院神経内科
3)旭川医科大学放射線科
4)富良野病院
5)旭川医科大学民工連携総合講座
(2010年8月30日受付，2010年9月28日受理)

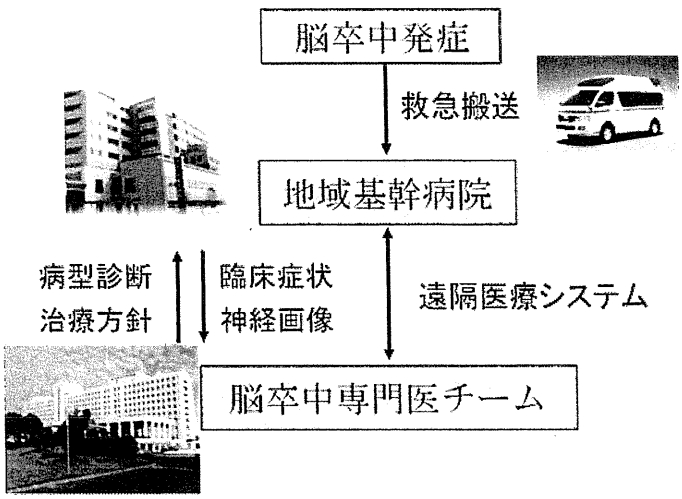

図1　Telestroke(脳卒中遠隔医療)の概念図

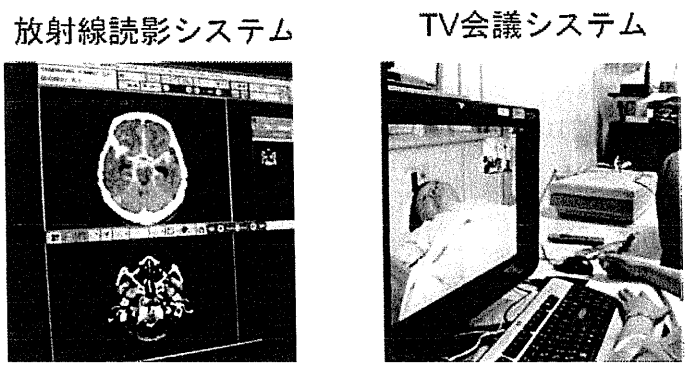

図2　放射線読影システムとTV会議システム
放射線読影システムにより地域基幹病院で撮像された画像を大学病院へ転送する．TV会議システムにより脳卒中患者の状態をリアルタイムで観察でき，地域基幹病院のスタッフあるいは患者自身とも会話ができる．

TV会議システムにはTandberg 880MXPを用い，通信回線にはNTT光回線(Bフレッツ)とセキュリティーのためフレッツVPNを使用した．ビットレートは1152 kbpsで，フレームレートは30フレーム/秒，解像度は4CIF(704×576ピクセル)，映像圧縮方式はH.264，音声符号化方式はG.722，TVモニターは20型デジタル液晶TV(シャープAQUOS)を用いた．音声は880MXPの機能で映像と同時に伝送し，マイクは880MXP内蔵，スピーカーはTVモニター内蔵を使用した．ビデオカメラはキャスター付台に載せて移動が自由に行えるようにした．放射線画像伝送システムにはTV会議システムとは別の光回線とVPNを使用した．

富良野病院と旭川医科大学とは既に放射線画像伝送システムを整備し遠隔画像診断が可能な体制にして，富良野病院で撮像されたCTやMRIなどの画像は旭川医科大学放射線科に転送され，画像診断を行えるようにした．すなわちリアルタイム型の脳卒中診療支援を行えるようにした．

臨床所見と放射線画像読影システムで転送された画像所見を合わせ，脳卒中の臨床診断を行い，治療方針を決定した．今回，初めてのシステム運用のため日中

表1　Telestroke症例のまとめ

	年齢	性	病名	症状	入院科	発症から富良野病院まで	富良野受診から当院まで	治療	転帰
No. 1	75	M	くも膜下出血	意識障害	当院脳神経外科	30 min	1h	保存的	当院へ転院，死亡
No. 2	66	M	被髄脈洞血栓症	けいれん	当院神経内科	30 min	3d	ヘパリン	当院へ転院，軽快後悪化
No. 3	75	M	心原性脳塞栓	歩行障害	当院神経内科	18h	5h	エダラボン，ヘパリン	当院へ転院，軽快
No. 4	81	M	視床出血	半身の異常感覚	近医脳外科出張病院	3d		降圧	近医転院，軽快
No. 5	76	M	外傷性くも膜下出血	頭痛	近医脳外科出張病院	30 min		保存的	近医転院，軽快
No. 6	62	M	ラクナ梗塞	半身の異常感覚	当院神経内科	2d	1h	エダラボン，オザグレル	当院へ転院，軽快
No. 7	65	F	くも膜下出血	頭痛	当院脳神経外科	1d	2.5h	クリッピング	当院へ転院，治癒
No. 8	81	F	多発性脳塞栓	右不全麻痺，構音障害	富良野病院	3h		エダラボン，ヘパリン	入院，軽快

のみに限定して開始した．2009年10月から2010年2月までの5カ月間に富良野病院へ救急搬送された脳卒中を疑われた8症例を対象とした．診断，治療，転帰，ならびに時間経過を検討し，telestrokeの有用性と課題を検討した．

結　果

8症例のまとめを表1に示した．Telestrokeを用いることにより，旭川医科大学において富良野病院に搬送された患者のバイタルサイン，意識状態，神経所見を明瞭にかつリアルタイムで確認することができた．ズームによる観察も可能で患者の表情の詳細まで把握できた．また患者と直接会話し，発語異常の有無や口頭指示による反応を確認することができた．同時に富良野病院で撮像されたCTやMRI，MRAを読影することができた．いずれの症例も富良野病院でtelestrokeにより診断を確定し治療方針と治療場所の決定を行った．8例中，5例は最終的に当院へ搬送し，2例は脳神経外科医が出張している富良野の近医へ転院した．1例は富良野病院で加療を継続した．すなわち4割弱が地域の医療機関で加療した．脳梗塞は3例で，発症から富良野病院搬入までの時間が最短で3時間，最長2日であり，t-PAの適応のある症例はいなかった．

二次搬送された5症例のうち症例3と症例6は脳梗塞で治療を開始して搬送したが，静脈洞血栓症の症例2は二次搬送した後に治療を開始した．残りの2例はくも膜下出血で，降圧療法を開始して搬送した．

富良野病院から当院までは救急車を用いると約1時間を要する．したがってtelestrokeを使用することにより診断および治療開始まで約1時間短縮すると考えられた．富良野病院から当院へ搬送された患者のうち2例は救急車を使用し約1時間で到着したが，他の2例はそれぞれ2時間と5時間を要した．その原因としては富良野病院受診時に救急車を使用せず，その後当院へ受診する際にも救急車を使用しなかったためと考えられた．当院へ搬送された患者に関しては受け入れ態勢の整備が前もって可能であった．

考　察

今回の検討でTV会議システムと放射線画像伝送システムを用いることにより，少数例ながらリアルタイムのtelestrokeを行うことができた．Telestrokeを用いることにより，これらの症例の診断から治療方針決定までの時間短縮は富良野病院から大学病院までの搬送時間である約1時間と考えられた．

診断後は富良野病院で加療を受けた場合にはその場で治療が開始され，大学病院まで搬送された症例も一

部を除き治療を開始して搬送された．

また，今まで富良野市で発症した脳卒中患者は主に脳卒中専門医のいる旭川市へ搬送されていたが，一部の例は富良野の医療機関で適切に治療まで行うことができたことは搬送費用や家族の交通費など診療以外に付随する費用の軽減につながるものと思われた．

1995年に発表されたNational Institute of Neurological Disorders and Stroke (NINDS) rt-PA Stroke Study trial[6]で3時間以内のt-PA静注療法が脳梗塞の3カ月後の機能予後の改善に有効とされてから，t-PA治療は脳梗塞発症から3時間以内の使用が原則である．今回は症例数が少なく適応症例がいなかったが，症例数が増加するに従い適応症例が見込まれると思われる．最近ではt-PAの使用が4.5時間まで延長しても有効との報告が相次いでおり[7]~[9]，今後，適応症例が拡大される可能性も示唆されている．しかし，発症から受診までの時間が長く，t-PA治療の適応時間を過ぎる例が多いことを考慮すると，脳卒中に関する知識を一般の方へ周知することがより重要な課題と考えられる．

今回の検討ではt-PA静注用法の適応症例がいなかったため，実際にこのシステムがt-PA静注療法に有用かどうかについては明らかでない．富良野病院でNIHSSスコアの正確な評価ができるか，t-PA静注療法に必要な問診や検査が適切に行えるかについて実証する必要がある．また，富良野病院でt-PA投与が可能であれば，救急隊から直接にt-PA可能な遠隔地への搬送(ストロークバイパス)より有効である可能性が高まると思われる．

富良野病院より当院へ搬送，受診するために要する時間が予測以上に長い症例に関しては，脳卒中が救急疾患であるとの認識の周知が徹底していなかった可能性があり，反省すべきものと考えられる．また救急車に加えドクターヘリなどの活用も搬送時間を短縮する有用な手段であり，考慮すべきものと考えられる．

Telestrokeによる富良野病院の利点として脳卒中専門医による診療あるいはコンサルトをいつでも受けられ，必要に応じ脳卒中専門医のいる大学病院への転院が可能であること，さらにそれにより地域基幹病院医師・患者・患者家族の安心感がえられることが考えられた．

Telestrokeの問題点の一つとしては，従事した病院への診療点数が算定されないことがある．今後telestrokeを進めるにあたり解決すべき課題と考えられる．Telestrokeの意義および有用性については脳卒中専門医のいない地域での脳卒中診療レベルの向上のみならず，患者自身の運搬費用と家族の交通費などの波及する医療経済学的観点，さらには機能予後の改善効果などを含め総合的に検証していく必要があると考えられる．

結　論

Telestrokeは脳卒中専門医のいない地域基幹病院での脳卒中診療に有用である．

謝　辞

Telestrokeの構築にご支援いただきました旭川医科大学学長吉田晃敏先生に深謝いたします．

本研究の一部は第35回日本脳卒中学会総会(2010年4月，盛岡)で発表した．

参考文献

1) Langhorne P, Williams BO, Gilchrist W, et al: Do stroke units save lives? Lancet 342: 395–398, 1993
2) Kaste M, Palomäki H, Sarna S: Where and how should elderly strokepatients be treated? A randomized trial. Stroke 26: 249–253, 1995
3) Collaborative systematic review of the randomised trials of organised inpatient (stroke unit) care after stroke. Stroke Unit Trialists' Collaboration. BMJ 314: 1151–1159, 1997
4) Kalra L, Evans A, Perez I, et al: Alternative strategies for stroke care: a prospective randomised controlled trial. Lancet 356: 894–899, 2000
5) Demaerschalk BM, Miley ML, Kiernan TE, et al; STARR Coinvestigators: Stroke telemedicine. Mayo Clin Proc 84: 53–64, 2009 (Erratum in: Mayo Clin Proc 85: 400, 2010)
6) The National Institute of Neurological Disorders and Stroke rt-PA Stroke Study Group: Tissue plasminogen activator for acute ischemic stroke. N Engl J Med 333: 1581–1587, 1995
7) Hacke W, Kaste M, Bluhmki E, et al for the ECASS investigators: Thrombolysis with alteplase 3 to 4.5 hours after acute ischemic stroke. N Engl J Med 359: 1317–1329, 2008
8) European Stroke Organization. ESO GC Statement on revised guidelines for intravenous thrombolysis. January 2009. Available at: http://www.eso-stroke.org pdf ESO. Accessed 15 May 2009
9) Bayley M, Lindsay P, Hellings C, et al, Canadian Stroke Strategy (a joint initiative of the Canadian Stroke Network and the Heart and Stroke Foun-

dation of Canada): Balancing evidence and opinion in stroke care: the 2008 best practice recommendations. CMAJ 179: 1247–1249, 2008
10) del Zoppo GJ, Saver JL, Jauch EC, et al; on behalf of the American Heart Association Stroke Council: Expansion of the time window for treatment of acute ischemic stroke with intravenous tissue plasminogen activator: a science advisory from the American Heart Association/American Stroke Association. Stroke 40: 2945–2948, 2009

Abstract

Telestroke in clinical practice

Hitoshi Aizawa, M.D., Ph.D.[1)2)], Jun Sawada, M.D., Ph.D.[1)], Tsukasa Saito, M.D.[1)], Hisako Endo, M.D.[1)], Takayuki Katayama, M.D., Ph.D.[1)], Naoyuki Hasebe, M.D., Ph.D.[1)], Hatsune Hiranuma, M.D., Ph.D.[3)], Kouji Takahashi, M.D., Ph.D.[3)], Syun Haneda, M.D., Ph.D.[4)] and Kiyoshi Moriya, Ph.D.[5)]

[1)]Division of Neurology, Department of Internal Medicine, Asahikawa Medical University
[2)]Present affiliation: Department of Neurology, Tokyo National Hospital, National Hospital Organization
[3)]Department of Radiology, Asahikawa Medical University
[4)]Furano Hospital
[5)]Department of Medicine and Engineering Combined Research Institute, Asahikawa Medical University

Background and Purpose: To examine whether a telestroke system is an effective method of providing expert stroke care to patients in rural areas.

Methods: Videoconferencing and radiological imaging linked the stroke center of Asahikawa Medical University Hospital and the emergency room of Furano Hospital (a rural hospital without access to a stroke specialist). The stroke patients referred to Furano Hospital were diagnosed using the telestroke system and started on medication. The clinical courses and outcomes of the patients were reviewed.

Results: A stroke specialist at a university hospital obtained clinical information on stroke patients at Furano Hospital through the videoconferencing system and viewed brain MRI/MRA/CT images of the patients. As a result, the time from the onset to starting treatment for the stroke patients was shortened.

Conclusions: The telestroke system is a useful tool for rural stroke medicine.

(Jpn J Stroke 33: 84–88, 2011)

Acta Neuropathol
DOI 10.1007/s00401-010-0678-x

ORIGINAL PAPER

TDP-43 pathology in sporadic ALS occurs in motor neurons lacking the RNA editing enzyme ADAR2

Hitoshi Aizawa · Jun Sawada · Takuto Hideyama · Takenari Yamashita · Takayuki Katayama · Naoyuki Hasebe · Takashi Kimura · Osamu Yahara · Shin Kwak

Received: 20 October 2009 / Revised: 28 February 2010 / Accepted: 20 March 2010

Abstract Both the appearance of cytoplasmic inclusions containing phosphorylated TAR DNA-binding protein (TDP-43) and inefficient RNA editing at the GluR2 Q/R site are molecular abnormalities observed specifically in motor neurons of patients with sporadic amyotrophic lateral sclerosis (ALS). The purpose of this study is to determine whether a link exists between these two specific molecular changes in ALS spinal motor neurons. We immunohistochemically examined the expression of adenosine deaminase acting on RNA 2 (ADAR2), the enzyme that specifically catalyzes GluR2 Q/R site-editing, and the expression of phosphorylated and non-phosphorylated TDP-43 in the spinal motor neurons of patients with sporadic ALS. We found that all motor neurons were ADAR2-positive in the control cases, whereas more than half of them were ADAR2-negative in the ALS cases. All ADAR2-negative neurons had cytoplasmic inclusions that were immunoreactive to phosphorylated TDP-43, but lacked non-phosphorylated TDP-43 in the nucleus. Our results suggest a molecular link between reduced ADAR2 activity and TDP-43 pathology.

Keywords Amyotrophic lateral sclerosis · Adenosine deaminase acting on RNA 2 · TDP-43 · RNA editing · Motor neuron

Electronic supplementary material The online version of this article (doi: [illegible]) contains supplementary material, which is available to authorized users.

H. Aizawa · J. Sawada · T. Katayama · N. Hasebe
Division of Neurology, Department of Internal Medicine, Asahikawa Medical College, 2-1-1-1 Midorigaoka-higashi, Asahikawa 078-8510, Japan

T. Hideyama · T. Yamashita · S. Kwak (✉)
CREST, Japan Science and Technology Agency, Department of Neurology, Graduate School of Medicine, The University of Tokyo, 7-3-1, Hongo, Bunkyo-ku, Tokyo 113-8655, Japan
e-mail: kwak-tky@umin.net

T. Kimura · O. Yahara
Department of Neurology, Douhoku National Hospital, Asahikawa, Japan

Introduction

Amyotrophic lateral sclerosis (ALS) is a devastating disease characterized by a progressive deterioration of motor function resulting from the degeneration of motor neurons. More than 90% of ALS cases are sporadic and approximately 5–10% are familial. Although at least six causal genes have been identified so far in individuals affected with familial ALS, SOD1 [40], ALS2 (alsin) [10, 39], senataxin (ALS4) [7], vesicle-trafficking protein/synaptobrevin-associated membrane protein [27], TAR DNA-binding protein (TDP-43) [9, 15, 32, 37, 40] and FUS/TLS [22, 35], the pathogenesis of sporadic ALS remains largely unexplored.

One hypothesis for selective neuronal death in sporadic ALS is excitotoxicity mediated by abnormally Ca^{2+}-permeable α-amino-3-hydroxy-5-methyl-4-isoxazolepropionate (AMPA) receptors, which are a subtype of the ionotropic glutamate receptor [6, 20, 21]. The recent finding of reduced RNA editing of the AMPA receptor subunit GluR2 at the Q/R site provides a plausible pathogenic mechanism underlying motor neuron death in sporadic ALS [16, 21, 34]. Reduced GluR2 Q/R site-editing, catalyzed by an

Published online: 07 April 2010

enzyme called adenosine deaminase acting on RNA 2 (ADAR2), appears to be specific to sporadic ALS among several neurodegenerative diseases [1, 19, 20, 29, 35].

TDP-43 was identified as a component of ubiquitin-positive, but tau-negative cytoplasmic inclusions in cortical neurons in patients with frontotemporal lobar degeneration (FTD) and spinal motor neurons in patients with sporadic ALS [5]. The TDP-43 found in these inclusions was demonstrated to be abnormally phosphorylated [12, 26].

Because both reduced GluR2 Q/R site-editing and formation of TDP-43-containing inclusions occur specifically in sporadic ALS motor neurons, we used immunohistochemistry to examine the expression of TDP-43 and ADAR2 in ALS motor neurons and elucidate a link between these two molecules.

Materials and methods

Subjects

This study was conducted using lumbar spinal cords from seven cases of sporadic ALS and six disease-free control cases. Consent for autopsy and approval for the use of human tissue specimens for research purposes was approved by appropriate institutional human ethics committees. Clinical information is given in Table 1.

Western blot analysis using the anti-ADAR2 antibody (RED1)

To examine the specificity of the polyclonal anti-ADAR2 antibody (RED 1) (Exalpha Biologicals, Watertown, MA) in the human brain, Western blot analysis was performed as reported previously [17]. From 100 mg of human frontal cortex, nuclear and cytoplasmic fractions were separated with the PARIS Protein and RNA Isolation System (TAKARA, Tokyo) according to the manufacturer's instructions. Nuclear and cytoplasmic proteins as well as those containing recombinant ADAR2a (rADAR2a) and recombinant ADAR2b (rADAR2b) proteins synthesized by in vitro translation were suspended in 500 μl of cold Cell Fraction Buffer provided with the PARIS Protein and RNA Isolation System (TAKARA). Samples were then boiled with 500 μl of 2 × SDS gel-loading buffer and subjected to SDS-PAGE. After electrophoresis, proteins were transferred to an Immobilon-P transfer membrane (Millipore, Bedford, MA). Blots were blocked in a buffer containing Tween/PBS and 1% bovine serum albumin (BSA). Then immunoblotting for histone protein (MAB052; CHEMICON, Temecula, CA, 1:2,000), glyceraldehyde-3 phosphate dehydrogenase (GAPDH) (MAB374; CHEMICON, 1:2,000) or ADAR2 (RED1; Exalpha Biologicals, Watertown, MA, 1:4,000) was conducted overnight at 4°C. For secondary antibodies, peroxidase-conjugated AffiniPure goat anti-mouse IgG (H + L) (Jackson ImmunoResearch, West Grove, PA; 1:5,000) or peroxidase-conjugated AffiniPure rabbit anti-sheep IgG (H + L) (Jackson ImmunoResearch; 1:5,000) was used. Visualization was carried out using ECL plus Western blotting detection reagents (GE Healthcare Bioscience, Piscataway, NJ). Specific bands were detected with an LAS 3000 system (Fujifilm, Tokyo).

Immunohistochemical analysis

The human spinal cords were fixed in 10% neutral buffered formalin for about 7 days and then embedded in paraffin. Serial 7 μm sections were cut for immunohistochemical analysis. The immunoreactive features of the anti-ADAR2 antibody on frozen sections were also evaluated. To examine the localization of ADAR2 and TDP-43 in a single neuron, a pair of adjacent sections was used for immunohistochemistry. The sections were mounted on slides and then deparaffinized in xylene, hydrated with an ethanol series and heated at 120°C for 2 min for antigen retrieval. The sections were then washed with phosphate-buffered saline (PBS) and incubated with the primary antibody overnight at 4°C. Polyclonal anti-ADAR2 (RED1, 1:100), monoclonal anti-phosphorylated TDP-43 (pTDP-43) (pS409/410) (Cosmo Bio Co., Ltd., Tokyo, Japan; 1:3,000) and rabbit polyclonal phosphorylation-independent anti-TARDBP (piTDP-43) (Protein-Tech Group, Inc.; 1:3,000) were used. Bound antibodies were detected using an avidin–biotin–peroxidase complex kit (Vector Laboratories, Burlingame, CA, USA). Diaminobenzidine tetrahydrochloride was used as the chromogen, and the sections were lightly counterstained with hematoxylin. The RED1 antibody was incubated with 5 μg/μl of recombinant ADAR2 (Abnova Corp., Taiwan) at 4°C overnight. These samples were then subjected to immunohistochemistry for the preabsorption test.

To test the effects of fixation, the paraffin-embedding procedure and the postmortem delay on ADAR2 immunoreactivity, rat spinal cord samples were processed either immediately after removal (PMI-0) or after the spinal cords were held at room temperature for 6 h (PMI-6) or 24 h (PMI-24). Some samples were quickly frozen on dry ice, and the others were fixed in 10% buffered formalin after each treatment. The immunohistochemical process was the same as that used for the paraffin-embedded human sections, except that frozen sections were incubated with the primary antibody for 1 h at room temperature after washing with PBS.

Frozen sections of lumbar spinal cords from $SOD1^{G93A}$ transgenic mice at 24 and 35 weeks of age were also used for immunohistochemistry with anti-ADAR2 and anti-pTDP-43 antibodies.

Table 1 Profiles of ALS cases and disease controls

Case	Age	Sex	PMI (h)	Brain weight (g)	Diagnosis	Duration of ALS	Onset of ALS	Number of MN/AH mean ± SD	ADAR2 (+) pTDP-43 (−) MN/AH mean ± SD (%)	ADAR2 (−) pTDP-43 (+) MN/AH mean ± SD (%)	ADAR2 (+) pTDP-43 (+) MN/AH *n* (%)	Number of AH examined
1	67	M	3	1,390	ALS	1 year 1 month	UE	6.0 ± 2.6	1.3 ± 1.5 (20.8)	4.8 ± 2.4 (79.2)	0	4
2	59	F	5	1,290	ALS	1 year 9 months	UE	2.3 ± 1.2	0 ± 0 (0.0)	2.3 ± 0.5 (100)	0	4
3	69	M	3	1,430	ALS	2 years	UE	3.3 ± 1.5	2.3 ± 1.9 (69.6)	1.0 ± 0.8 (30.4)	0	7
4	75	F	2	1,080	ALS	2 years 6 months	LE	8.7 ± 3.1	5.7 ± 2.8 (65.4)	3.0 ± 3.0 (34.6)	1 (0.2)	6
5	72	M	1.5	1,290	ALS	3 years 1 month	Bulb	3.5 ± 1.6	0.5 ± 0.6 (14.3)	3.0 ± 1.2 (85.7)	0	4
6	62	M	3	1,390	ALS	3 years 7 months	UE	4.9 ± 1.7	1.3 ± 0.8 (26.5)	3.6 ± 1.7 (73.5)	0	7
7	69	M	1.5	1,460	ALS	12 years	UMN	2.2 ± 0.7	0.8 ± 0.4 (38.5)	1.3 ± 0.3 (61.5)	0	6
8	64	M	2	1,200	Cerebellar tumor			15.8 ± 8.6	15.8 ± 8.6 (100)	0	0	4
9	58	M	7	1,420	Myotonic dystrophy			13.3 ± 7.2	13.3 ± 7.2 (100)	0	0	4
10	70	F	2	1,040	Limb-girdle muscular dystrophy			10.2 ± 5.4	10.2 ± 5.4 (100)	0	0	6
11	73	M	3	1,170	Theophylline intoxication			8.2 ± 4.9	8.2 ± 4.9 (100)	0	0	6
12	77	M	1.5	1,200	Limb-girdle muscular dystrophy			10.9 ± 6.1	10.9 ± 6.1 (100)	0	0	8
13	78	M	1	1,310	Meningitis			8.4 ± 4.6	8.4 ± 4.6 (100)	0	0	8

PMI postmortem interval, *AH* anterior horn, *MN* motor neuron, *UE* upper extremities, *LE* lower extremities, *Bulb* bulbar symptoms, *UMN* upper motor neuron sign

Double immunofluorescence study using anti-ADAR2 antibody and anti-phosphorylation-independent TDP-43 antibody

Formalin-fixed paraffin-embedded spinal cord sections from an ALS patient (case 6 in Table 1) were double-immunostained with RED1 antibody (×100) and anti-TDP-43 monoclonal antibody (Abnova, ×1,000). Labeled goat anti-rabbit IgG antibody (Molecular Probes, Alexa 488) and labeled goat anti-mouse IgG (Molecular Probes, Alexa 594) were used as secondary antibodies (×1,000).

Quantification of motor neurons in ALS and control spinal cords

Serial sections of both ALS and control cases were immunostained with piTDP-43, ADAR2, or pTDP-43. Large ADAR2-positive and -negative neurons with nucleoli in the anterior horns on each section were counted separately. In addition, we examined whether each of the motor neurons was immunostained with pTDP-43 or piTDP-43 in the respective adjacent section.

Statistics

The Mann–Whitney *U* test was used to compare the number of anterior horn cells (AHC) in ALS samples compared to controls.

Results

Nuclear localization of ADAR2

The Western blot analysis of the human cortex showed that the anti-ADAR2 antibody (RED1) recognized two isoforms of active ADAR2 protein, ADAR2a and ADAR2b, in the nuclear fraction, but not in the cytoplasmic fraction. It is reasonable for ADAR2 to be localized in the nuclear fraction because ADAR2 primarily acts on RNA. The validity of this fractionation was verified by the presence of histone in the nuclear fraction and of GAPDH in the cytoplasmic fraction (Fig. 1a). ADAR2 immunoreactivity is observed in the nuclei of motor neurons from frozen sections of rat (Fig. 1b) and human spinal cords (Fig. 1c).

ADAR2 expression in motor neurons of normal rat and SOD1 transgenic mouse

Intense ADAR2 immunoreactivity was observed in the nucleolus of the nuclei from all motor neurons examined in the frozen rat sections (Fig. 2a, c), whereas both the nucleus and cytoplasm were immunoreactive for ADAR2

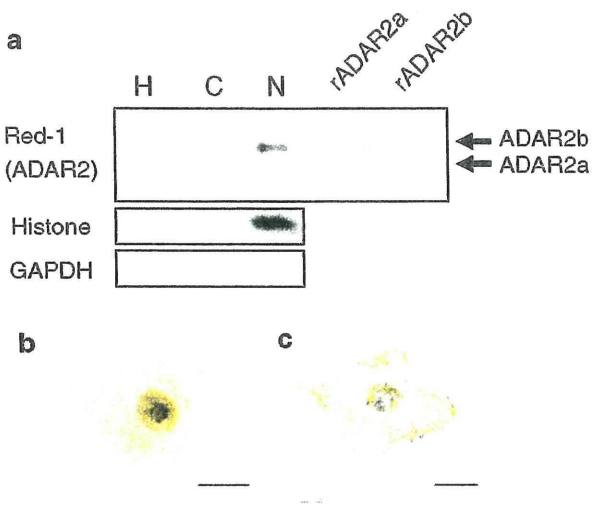

Fig. 1 Nuclear localization of the ADAR2 protein in the human brain. Western blot analysis of the human cortex demonstrates that ADAR2 protein is localized in the nuclear fraction, but not in the cytoplasmic fraction. The validity of this fractionation was verified by the presence of histone in the nuclear fraction and of GAPDH in the cytoplasmic fraction. ADAR2 immunoreactivity is demonstrated in the nuclei of large neurons in the anterior horn of the rat spinal cord (**b**) and the human spinal cord (**c**). *Bar* indicates 20 μm. *N* nuclear fraction, *C* cytoplasmic fraction, *H* brain homogenate, *rADAR2a* recombinant human ADAR2a, *rADAR2b* recombinant human ADAR2b

in the paraffin-embedded sections of both PMI-0 and PMI-6 tissues (Fig. 2b, d, e, g, h). The intensity of ADAR2 immunoreactivity varied markedly among the nuclei (even on the same section) and was uniformly low in the cytoplasm of the motor neurons in the paraffin-embedded sections. ADAR2 immunoreactivity in the nuclei of motor neurons on the frozen and paraffin-embedded sections of PMI-24 tissue was less intense than in PMI-0 and PMI-6 tissues (Fig. 2). ADAR2 immunoreactivity was observed in the nucleus of all the motor neurons examined in the spinal cords of $SOD1^{G93A}$ transgenic mice (Fig. 3b).

ADAR2, phosphorylation-dependent TDP-43 and phosphorylation-independent TDP-43 expression in human control spinal motor neurons

In the spinal cords of human control cases, all motor neurons examined ($n = 380$ from 6 cases) showed ADAR2 immunoreactivity, typically in the cytoplasm with slight or no apparent immunoreactivity observed in the nuclei (Table 1; Figs. 4a, b, 5a). Similar ADAR2 immunoreactivity was observed in all the neurons in the pontine nuclei, including atrophic neurons in patients with multiple system atrophy and spinocerebellar atrophy type 1 (Supplementary Figure 1). Phosphorylation-independent TDP-43 (piTDP-43) stained the nuclei of the same motor

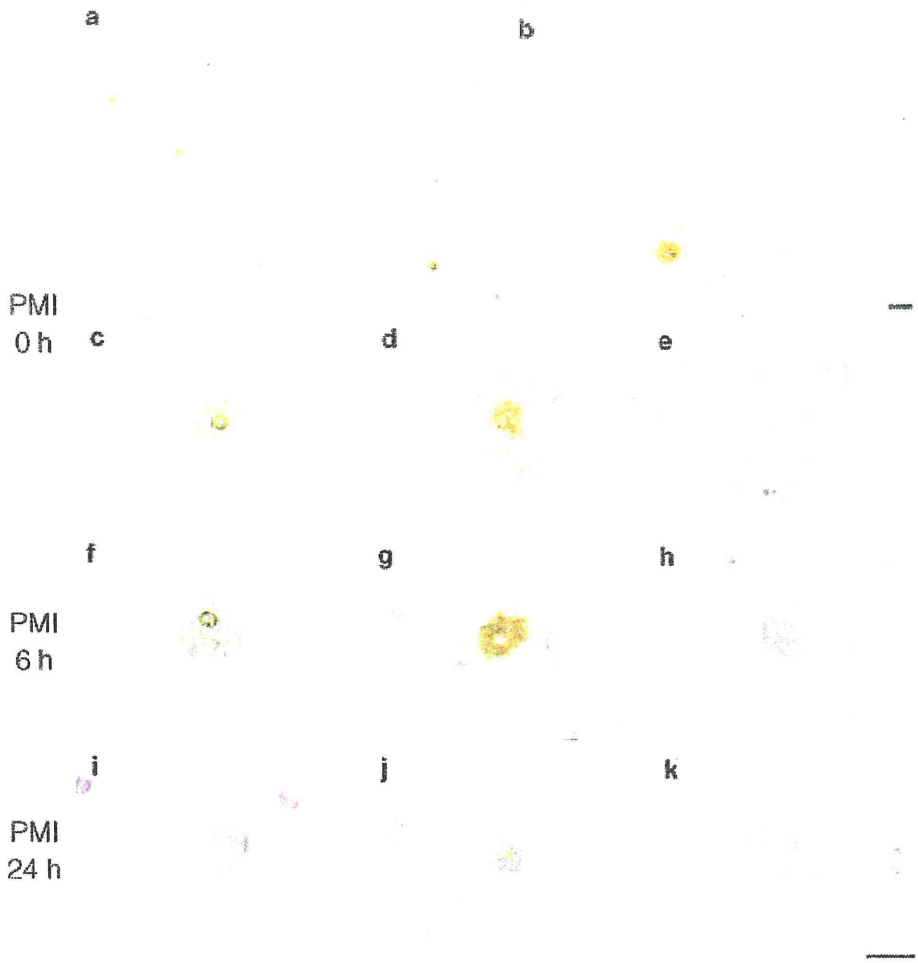

Fig. 2 ADAR2 immunohistochemistry of motor neurons in the rat lumbar spinal cord. ADAR2 is expressed in the nuclei of neurons in frozen sections created at 0 h postmortem (**a**, **c**). On the contrary, ADAR2 is always positive in the cytoplasm of neurons in formalin-fixed, paraffin-embedded sections from different rats, with a variable intensity of nuclear immunoreactivity among neurons (**b**, **d**, **e**). Frozen (**f**) and paraffin-embedded sections (**g**, **h**) with a 6-h postmortem interval display immunoreactivity similar to those with a 0-h postmortem interval. Nuclear immunoreactivity was less intense on both frozen sections (**i**) and paraffin-embedded sections (**j**, **k**) created at 24 h postmortem compared with those prepared at 0 h. *PM* postmortem interval. *Bar* indicates 20 μm

neurons (Figs. 4a′, a″, b′, 5b, c), while phosphorylation-dependent TDP-43 (pTDP-43) did not stain either the nucleus or cytoplasm on the adjacent section (Fig. 4b″). Two different anti-ADAR2 antibodies exhibited immunoreactivity in the cytoplasm of motor neurons (Fig. 4a, b, g, Supplementary Figure 2), and preabsorbed anti-ADAR2 antibody did not show any immunoreactivity (Fig. 4h).

ADAR2, pTDP-43 and piTDP-43 expression in ALS spinal motor neurons

Both ADAR2-positive (Fig. 4c open arrow) and -negative motor neurons (Fig. 4c closed arrow) were observed in the ALS spinal cords. The immunoreactivity in the ADAR2-positive neurons was observed in the cytoplasm, but apparently not in the nuclei (Figs. 4c open arrow, e, f, 5d, f), as observed in the control motor neurons. These ADAR2-positive neurons showed normal piTDP-43 immunoreactivity in the nucleus (Figs. 4e′, f′, 5e, f,), but exhibited no pTDP-43-positive inclusions (Fig. 4c, c′). In contrast, all ADAR2-negative neurons showed pTDP-43-positive inclusions in the cytoplasm (Fig. 4c′, d′).

Cell count of anterior horn motor neurons

The number of anterior horn cells (motor neurons) (AHC) in 7 sporadic ALS cases was reduced to 39 ± 21% (mean ± SD) of the number in control cases ($p < 0.0001$, Mann–Whitney's U test, Fig. 5). A significant proportion of motor neurons (98 out of 170 anterior horn cells; 58%) in the spinal cords obtained from patients with ALS were ADAR2-negative (Table 1; Fig. 6). ADAR2-negative motor neurons were observed in all ALS cases examined, but the proportions varied from 30% in case 3 to 100% in case 2 (Table 1). Notably, all the ADAR2-negative motor neurons had pTDP-43-positive inclusions in the cytoplasm. Conversely, virtually all the ADAR2-positive motor neurons had piTDP-43 immunoreactivity in their nuclei, but did not exhibit pTDP-43-positive cytoplasmic inclusions (Table 1; Fig. 6). Only one motor neuron was stained with

Fig. 3 Expression of ADAR2 and phosphorylation-dependent TDP-43 in spinal motor neurons of SOD1 transgenic mice. A low-magnification view of the lumbar spinal anterior horn in a $SOD1^{G93A}$ transgenic mouse, at 34 weeks of age showing that all the motor neurons are ADAR2 positive (**a**). A high-magnification view shows predominant nuclear immunoreactivity (**b**). There is no phosphorylation-dependent TDP-43 immunoreactive inclusion in the motor neurons (**c**, *arrow*). *Bar* indicates 20 μm

both ADAR2 and pTDP-43 ($n = 1$ in case 4), but none of the motor neurons lacked immunoreactivity to both ADAR2 and pTDP-43. These results indicate a strong association between ADAR2-deficiency and the development of pTDP-43-positive inclusions in the motor neurons of patients with sporadic ALS. However, there is no apparent relationship between the duration of disease and the number of remaining motor neurons with ADAR2 positivity and/or pTDP-43 positivity.

Discussion

ADAR2 expression was observed in all 380 spinal motor neurons examined in the control cases in this study, and in a portion of the spinal motor neurons from ALS cases (approximately 42% of 170 neurons). The nuclei of these ADAR2-positive neurons were also immunoreactive for piTDP-43. Notably, more than half the motor neurons in ALS cases lacked immunoreactivity to both ADAR2 and piTDP-43, but these double-negative neurons always displayed pTDP-43-positive inclusions in the cytoplasm. Therefore, normal motor neurons express ADAR2 without forming phosphorylated TDP-43-positive cytoplasmic inclusions, whereas motor neurons lacking ADAR2 in sporadic ALS formed inclusions.

ADAR2 immunoreactivity was exclusively observed in the nuclei of rat motor neurons on the frozen sections created 0–6-h postmortem. Because the density of motor neurons in the spinal ventral gray matter is too low to detect ADAR2 by Western blotting analysis, we used frozen human brain for the analysis, which demonstrated that RED1 specifically recognized two isoforms of active ADAR2 protein in the nuclear fraction [17]. The nuclear localization of the ADAR2 protein in the motor neurons was demonstrated immunohistochemically in frozen human spinal cord sections. In addition, expression of ADAR2 mRNA in the human spinal cord was demonstrated [18]. These results are consistent with the function of ADAR2 in the cell nucleus, which is catalysis of the conversion of adenosine to inosine (A-to-I) at various pre-mRNA positions including the Q/R site of GluR2. We also observed ADAR2 immunoreactivity in the cytoplasm of motor neurons in human paraffin-embedded sections. Importantly, the nuclei of motor neurons were predominantly immunoreactive to ADAR2 in frozen sections of the same control subject. In paraffin-embedded sections and frozen sections from the spinal cord after a 24-h postmortem interval, there was a reduction in ADAR2 immunoreactivity in the nucleus with the concomitant appearance of immunoreactivity in the cytoplasm of rat motor neurons. Therefore, ADAR2 immunoreactivity in the cytoplasm likely represented ADAR2 protein translocated from the nucleus to the cytoplasm resulting from the procedure of paraffin embedding and/or the delay between death and tissue fixation, which are unavoidable during routine neuropathological examinations of human autopsy materials. Because all the control motor neurons demonstrated cytoplasmic ADAR2 immunoreactivity, it is likely that ADAR2-negative motor neurons in ALS spinal cords lacked ADAR2 protein localized to the nucleus.

ADAR2 is involved in the A-to-I conversion of various pre-mRNAs and specifically catalyzes GluR2 Q/R site-editing. AMPA receptors containing GluR2 which is unedited at the Q/R site have significantly higher Ca^{2+} permeability than those containing edited GluR2. This factor plays a crucial role in neuron survival [5, 11]. Neurons in the mammalian brain only express Q/R site-edited GluR2 mRNA, and mice unable to edit this site die from status epilepticus early in life [14]. GluR2 Q/R site-editing occurs with 100% efficiency in normal human motor neurons, but is characterized by high variability (from 0 to 100%) among individual motor neurons in individual cases of ALS [19]. Therefore, ADAR2-positive

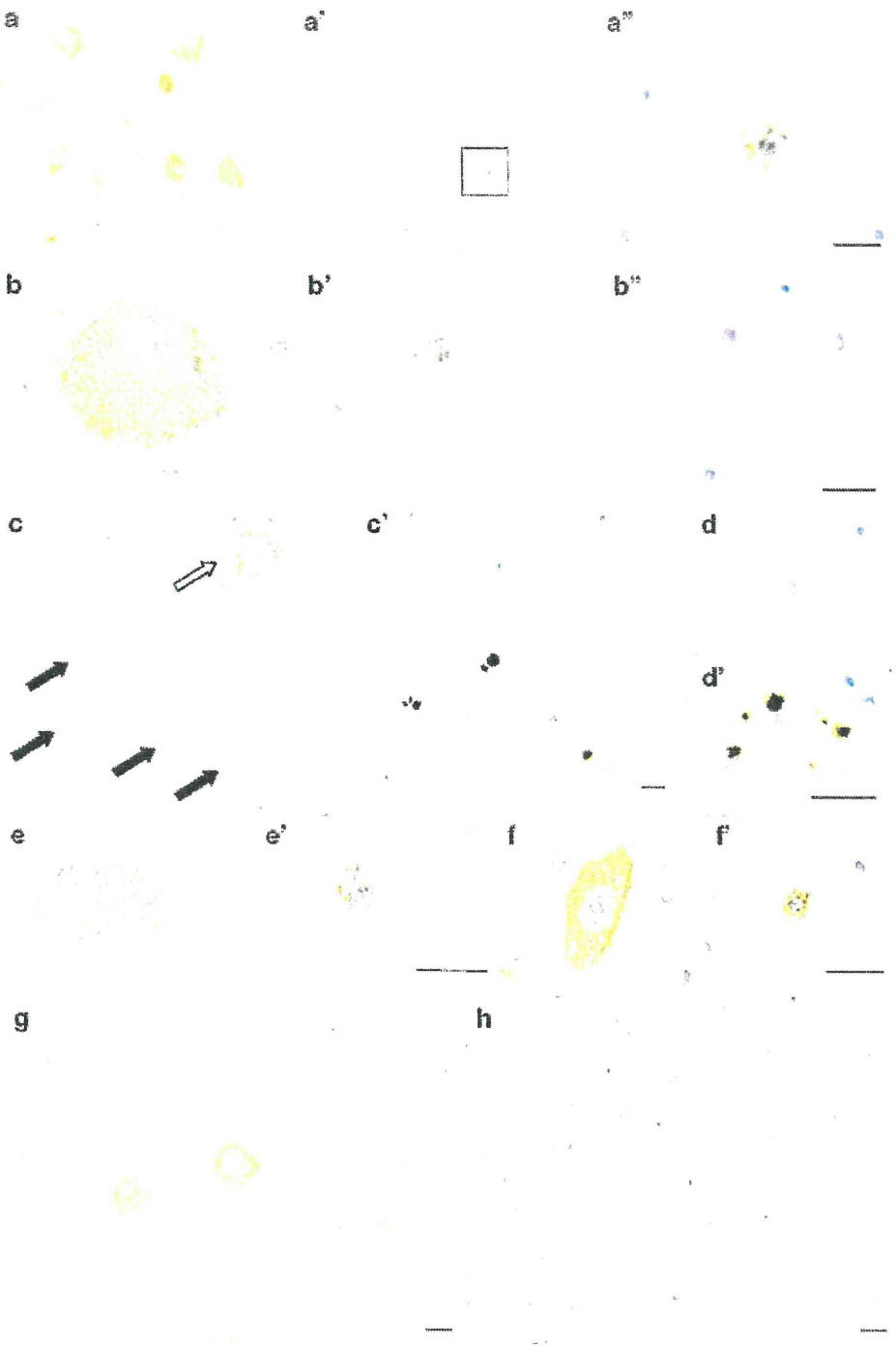

Fig. 4 Expression of ADAR2, phosphorylation-dependent TDP-43 and phosphorylation-independent TDP-43 in spinal motor neurons from adjacent sections. A low-magnification view of the lumbar spinal anterior horn in a control subject (case 8) shows that all the motor neurons are immunoreactive for ADAR2 (**a**). These neurons show phosphorylation-independent TDP-43 (piTDP-43) immunoreactivity in the nucleus in an adjacent section (**a′**, **a″**: a high-magnification view of the open square in **a′**). A lumbar spinal motor neuron from a control subject (case 12) shows diffuse ADAR2 immunoreactivity in the cytoplasm (**b**). The adjacent section shows piTDP-43 immunoreactivity in the nucleus (**b′**), but does not show phosphorylation-dependent TDP-43 (pTDP-43) immunoreactivity (**b″**). All ADAR2-negative neurons (*closed arrows* in *c*; case 6) display pTDP-43-positive inclusions in the cytoplasm (**c′**), whereas an ADAR2-positive neuron from a patient with ALS (*open arrow* in **c**) has no pTDP-43 immunoreactivity (**c′**). An ADAR2-negative neuron (**d**; case 6) has multiple pTDP-43-positive inclusions in the cytoplasm (**d′**). ADAR2-positive neurons (**e** case 6, **f** case 3) show phosphorylation-independent TDP-43 immunoreactivity in the nucleus (**e′**, **f′**). ADAR2 immunoreactivity in the cytoplasm (**g**) disappeared when recombinant ADAR2-preabsorbed anti-ADAR2 antibody was used as the primary antibody (**h**) (case 12). *Bar* indicates 20 μm

motor neurons likely represent normal neurons expressing Q/R site-edited GluR2, whereas ADAR2-negative motor neurons represent those expressing Q/R site-unedited GluR2 [16, 20]. The present results indicating the presence of both ADAR2-positive and -negative motor neurons are consistent with high variability in the efficiency of GluR2 Q/R site-editing (from 0 to 100%) among individual motor neurons in ALS patients [16]. These findings strengthen the hypothesis that reduced ADAR2 activity is closely associated with the pathogenesis of sporadic ALS [20].

The presence or absence of ADAR2 immunoreactivity in the cytoplasm of motor neurons was conversely related to pTDP-43 immunoreactivity in the cytoplasm. Abnormally processed TDP-43 was initially identified as a

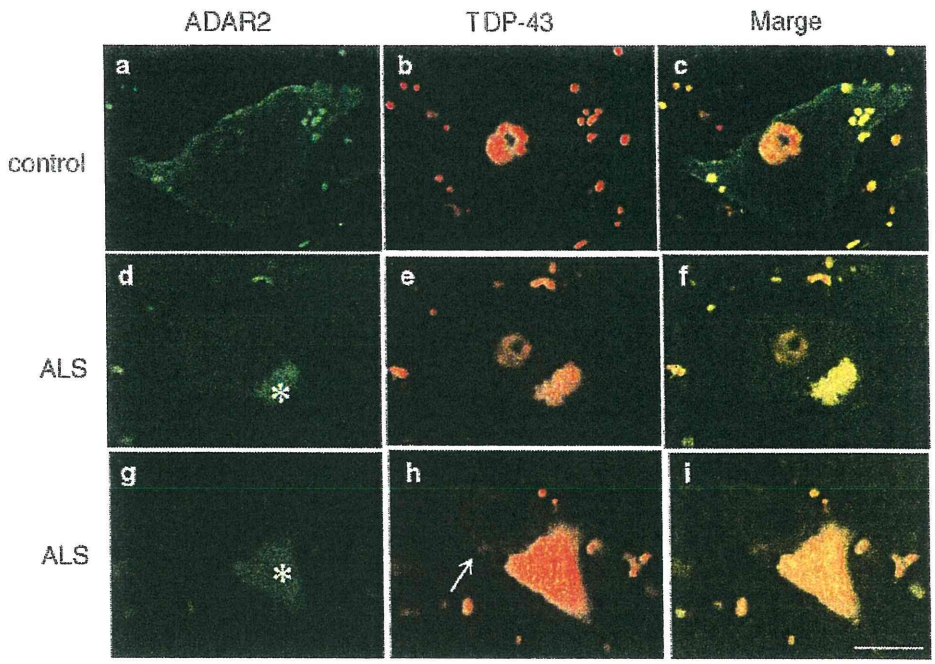

Fig. 5 Double-labeled immunofluorescence study using anti-ADAR2 and anti-piTDP-43 antibodies. **a–c** Control motor neuron was immunopositive for ADAR2 in the cytoplasm and nucleus and piTDP-43 in the nucleus. **d–f** An ALS motor neuron immunoreactive to ADARA2 in the cytoplasm showed immunoreactivity to piTDP-43 in the nucleus. **g–i** An ALS motor neuron lacking immunoreactivity to ADAR2 showed piTDP-43 positive cytoplasmic inclusions (*arrow*) and loss of piTDP-43 immunoreactivity in the nucleus. Asterisks indicate lipofuscin autofluorescence. *Bar* indicates 20 μm

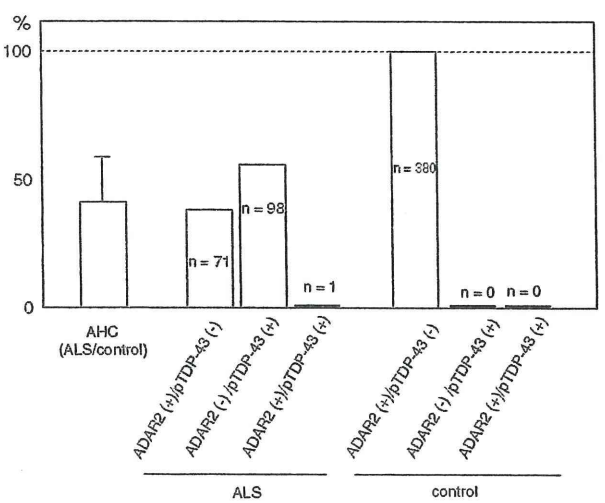

Fig. 6 Motor neurons with different immunoreactivities in ALS and control cases. The number of anterior horn cells (motor neurons) (AHCs) in 7 sporadic ALS cases was reduced to 39 ± 21% (mean ± SD) of the number in control cases ($p < 0.0001$, Mann–Whitney *U* test). In ALS cases, 42% of total AHCs were ADAR2-positive and pTDP-43-negative (*pink bar*); 58% were ADAR2-negative and pTDP-43-positive (*blue bar*). Only one AHC out of 170 (0.2%) was positive for both ADAR2 and pTDP-43, and none were negative for both ADAR2 and pTDP-43. All lumbar spinal motor neurons ($n = 380$) from 6 control cases were ADAR2-positive and pTDP-43-negative (*pink bar*). *AHC* anterior horn cell (motor neuron)

protein component of ubiquitin-positive and tau-negative inclusions in the brains of patients with FTD and ALS [3, 25]. Subsequently, abnormal TDP-43-positive inclusions were found in various proportions in neurons from patients with other neurodegenerative disorders, such as Parkinson's disease dementia and dementia with Lewy bodies [24], Parkinsonism-dementia complex and ALS in Guam [8, 11], corticobasal degeneration [26] and Alzheimer's disease [2, 13, 36]. These results imply that aberrant processing of TDP-43 may be involved in a common pathway of the neurodegenerative process and that the accumulation of pTDP-43 in the cytoplasm of motor neurons is not a disease-specific event in ALS [2, 13, 24, 36].

This study demonstrates that all ADAR2-negative motor neurons showed pTDP-43-positive inclusions in the cytoplasm in cases of sporadic ALS, suggesting a molecular association between reduced ADAR2 activity and the formation of pTDP-43-positive inclusions in ALS motor neurons. Both TDP-43 and ADAR2 are nuclear proteins, playing roles in the regulation of RNA processing; TDP-43 regulates RNA splicing [4, 28] and ADAR2 catalyzes RNA editing. However, there is no report regarding the functional link between the two molecules. We found that pTDP-43-positive inclusions showed no ADAR2 immunoreactivity, indicating that the trapping of ADAR2 protein in the inclusions due to direct protein–protein interaction is unlikely. Reduced ADAR2 activity increases Ca^{2+} permeable AMPA receptors by failure to edit the Q/R site of GluR2 [5, 6, 14], but it is not known whether an increase of the Ca^{2+} overload influences the TDP-43 processing. Thus, it is not clear from the present immunohistochemical study whether the reduced ADAR2 expression is a cause or a consequence of TDP-43 pathology. Interestingly, neither pTDP-43-positive inclusions [24, 35] nor a reduction of GluR2 Q/R-site-editing [19] was associated with

SOD1-related familial ALS or SBMA, an X-linked hereditary lower motor neuron disease associated with expanded CAG repeats in the androgen receptor gene. Consistent with the absence of pTDP-43-positive inclusions in the spinal motor neurons of *SOD1*-associated familial ALS, present study demonstrated that all the motor neurons examined were ADAR2-positive in $SOD1^{G93A}$ transgenic mouse spinal cords. Elucidation of the molecular mechanism underlying the co-occurrence of reduced ADAR2 activity and abnormal TDP-43 pathology in the same motor neurons may provide a clue to the neurodegenerative process of sporadic ALS.

References

1. Akbarian S, Smith MA, Jones EG (1995) Editing for an AMPA receptor subunit RNA in prefrontal cortex and striatum in Alzheimer's disease, Huntington's disease and schizophrenia. Brain Res 699:297–304
2. Amador-Ortiz C, Lin WL, Ahmed Z et al (2007) TDP-43 immunoreactivity in hippocampal sclerosis and Alzheimer's disease. Ann Neurol 61:435–445
3. Arai T, Hasegawa M, Akiyama H et al (2006) TDP-43 is a component of ubiquitin-positive tau-negative inclusions in frontotemporal lobar degeneration and amyotrophic lateral sclerosis. Biochem Biophys Res Commun 351:602–611
4. Buratti E, Baralle FE (2008) Multiple roles of TDP-43 in gene expression, splicing regulation, and human disease. Front Biosci 13:867–878
5. Burnashev N, Monyer H, Seeburg PH, Sakmann B (1992) Divalent ion permeability of AMPA receptor channels is dominated by the edited form of a single subunit. Neuron 8:189–198
6. Carriedo SG, Yin HZ, Weiss JH (1996) Motor neurons are selectively vulnerable to AMPA/kainate receptor-mediated injury in vitro. J Neurosci 16:4069–4079
7. Chen YZ, Bennett CL, Huynh HM et al (2004) DNA/RNA helicase gene mutations in a form of juvenile amyotrophic lateral sclerosis (ALS4). Am J Hum Genet 74:1128–1135
8. Geser F, Winton MJ, Kwong LK et al (2008) Pathological TDP-43 in parkinsonism-dementia complex and amyotrophic lateral sclerosis of Guam. Acta Neuropathol 115:133–145
9. Gitcho MA, Baloh RH, Chakraverty S et al (2008) TDP-43 A315T mutation in familial motor neuron disease. Ann Neurol 63:535–538
10. Hadano S, Hand CK, Osuga H et al (2001) A gene encoding a putative GTPase regulator is mutated in familial amyotrophic lateral sclerosis 2. Nat Genet 29:166–173
11. Hasegeawa M, Arai T, Akiyama H et al (2007) TDP-43 is deposited in the Guam Parkinsonism-dementia complex brains. Brain 130:1386–1394
12. Hasegawa M, Arai T, Nonaka T et al (2008) Phosphorylated TDP-43 in frontotemporal lobar degeneration and amyotrophic lateral sclerosis. Ann Neurol 64:60–70
13. Higashi S, Iseki E, Yamamoto R et al (2007) Concurrence of TDP-43, tau and alpha-synuclein pathology in brains of Alzheimer's disease and dementia with Lewy diseases. Brain Res 1184:284–394
14. Higuchi M, Maas S, Single FN et al (2000) Point mutation in an AMPA receptor gene rescues lethality in mice deficient in the RNA-editing enzyme ADAR2. Nature 406:78–81
15. Kabashi E, Valdmanis PN, Dion P et al (2008) TARDBP mutations in individuals with sporadic and familial amyotrophic lateral sclerosis. Nat Genet 40:572–574
16. Kawahara Y, Ito K, Sun H et al (2004) Glutamate receptors: RNA editing and death of motor neurons. Nature 427:801
17. Kawahara Y, Ito K, Ito M, Tsuji S, Kwak S (2005) Novel splice variants of human ADAR2 mRNA: skipping of the exon encoding the dsRNA-binding domains, and multiple C-terminal splice sites. Gene 363:193–201
18. Kawahara Y, Kwak S (2005) Excitotoxicity and ALS: what is unique about the AMPA receptors expressed on spinal motor neurons? Amyotroph Lateral Scler Other Motor Neuron Disord 6:131–144
19. Kawahara Y, Sun H, Ito K et al (2006) Underediting of GluR2 mRNA, a neuronal death inducing molecular change in sporadic ALS, does not occur in motor neurons in ALS1 or SBMA. Neurosci Res 54:11–14
20. Kwak S, Kawahara Y (2005) Deficient RNA editing of GluR2 and neuronal death in amyotropic lateral sclerosis. J Mol Med 83:110–120
21. Kwak S, Weiss JH (2006) Calcium-permeable AMPA channels in neurodegenerative disease and ischemia. Curr Opin Neurobiol 16:281–287
22. Kwiatkowski TJ Jr, Bosco DA, Leclerc AL et al (2009) Mutations in the FUS/TLS gene on chromosome 16 cause familial amyotrophic lateral sclerosis. Science 323:1205–1208
23. Mackenzie IR, Bigio EH, Ince PG et al (2007) Pathological TDP-43 distinguishes sporadic amyotrophic lateral sclerosis from amyotrophic lateral sclerosis with SOD1 mutations. Ann Neurol 61:427–434
24. Nakashima-Yasuda H, Uryu K, Robinson J et al (2007) Co-morbidity of TDP-43 proteinopathy in Lewy body related diseases. Acta Neuropathol 114:221–229
25. Neumann M, Sampathu DM, Kwong LK et al (2006) Ubiquitinated TDP-43 in frontotemporal lobar degeneration and amyotrophic lateral sclerosis. Science 314:130–133
26. Neumann M, Kwong LK, Lee EB et al (2009) Phosphorylation of S409/410 of TDP-43 is a consistent feature in all sporadic and familial forms of TDP-43 proteinopathies. Acta Neuropathol 117:137–149
27. Nishimura AL, Mitne-Neto M, Silva HC et al (2004) A mutation in the vesicle-trafficking protein VAPB causes late-onset spinal muscular atrophy and amyotrophic lateral sclerosis. Am J Hum Genet 75:822–831
28. Ou SH, Wu F, Harrich D et al (1995) Cloning and characterization of a novel cellular protein, TDP-43, that binds to human immunodeficiency virus type 1 TAR DNA sequence motifs. J Virol 69:3584–3596
29. Paschen W, Hedreen JC, Ross CA (1994) RNA editing of the glutamate receptor subunits GluR2 and GluR6 in human brain tissue. J Neurochem 63:1596–1602
30. Rosen DR, Siddique T, Patterson D et al (1993) Mutations in Cu/Zn superoxide dismutase gene are associated with familial amyotrophic lateral sclerosis. Nature 362:59–62
31. Sommer B, Köhler M, Sprengel R, Seeburg PH (1991) RNA editing in brain controls a determinant of ion flow in glutamate-gated channels. Cell 67:11–19
32. Sreedharan J, Blair IP, Tripathi VB et al (2008) TDP-43 mutations in familial and sporadic amyotrophic lateral sclerosis. Science 319:1668–1672
33. Suzuki T, Tsuzuki K, Kameyama K, Kwak S (2003) Recent advances in the study of AMPA receptors. Nippon Yakurigaku Zasshi 122:515–526
34. Takuma H, Kwak S, Yoshizawa T, Kanazawa I (1999) Reduction of GluR2 RNA editing, a molecular change that increases calcium influx through AMPA receptors, selective in the spinal

ventral gray of patients with amyotrophic lateral sclerosis. Ann Neurol 46:806–815
35. Tan CF, Eguchi H, Tagawa A et al (2007) TDP-43 immunoreactivity in neuronal inclusions in familial amyotrophic lateral sclerosis with or without SOD1 gene mutation. Acta Neuropathol 113:535–542
36. Uryu K, Nakashima-Yasuda H, Forman MS et al (2008) Concomitant TAR-DNA-binding protein 43 pathology is present in Alzheimer disease and corticobasal degeneration but not in other tauopathies. J Neuropathol Exp Neurol 67:555–564
37. Van Deerlin VM, Leverenz JB, Bekris LM et al (2008) TARDBP mutations in amyotrophic lateral sclerosis with TDP-43 neuropathology: a genetic and histopathological analysis. Lancet Neurol 7:409–416
38. Vance C, Rogelj B, Hortobágyi T et al (2009) Mutations in FUS, an RNA processing protein, cause familial amyotrophic lateral sclerosis type 6. Science 323:1208–1211
39. Yang Y, Hentati A, Deng HX et al (2001) The gene encoding alsin, a protein with three guanine-nucleotide exchange factor domains, is mutated in a form of recessive amyotrophic lateral sclerosis. Nat Genet 29:160–165
40. Yokoseki A, Shiga A, Tan CF et al (2008) TDP-43 mutation in familial amyotrophic lateral sclerosis. Ann Neurol 63:538–542